

Pressure effects on relaxor ferroelectricity in disordered $\text{Pb}(\text{Sc}_{1/2}\text{Nb}_{1/2})\text{O}_3$

Muhtar Ahart,^{1,a)} Ho-kwang Mao,¹ R. E. Cohen,¹ Russell J. Hemley,¹
George A. Samara,^{2,b)} Yonghong Bing,³ Zuo-Guang Ye,³ and Seiji Kojima⁴

¹*Geophysical Laboratory, Carnegie Institution of Washington, Washington, DC 20015, USA*

²*Sandia National Laboratory, Albuquerque, New Mexico 87175, USA*

³*Department of Chemistry and 4D LABS, Simon Fraser University, Burnaby, BC V5A 1S6, Canada*

⁴*Institute of Materials Science, University of Tsukuba, Tsukuba, Ibaraki 305-8573, Japan*

(Received 3 December 2009; accepted 18 February 2010; published online 15 April 2010)

High-pressure Brillouin and Raman scattering spectroscopy and x-ray diffraction measurements were carried out on disordered $\text{Pb}(\text{Sc}_{1/2}\text{Nb}_{1/2})\text{O}_3$, considered to be a model system for phase transitions in relaxor ferroelectrics and related materials. The observed pressure-dependent Raman spectra are unusual, with the relaxor state distinguished by broad Raman bands. Raman spectra as a function of pressure reveal a new peak at 370 cm^{-1} , with two peaks near 550 cm^{-1} merge above 2–3 GPa, indicating a structural phase transition in this pressure range consistent with earlier dielectric measurements. A significant softening in the longitudinal acoustic mode is observed by Brillouin scattering. Both the temperature and pressure dependencies of the linewidth reveal that the longitudinal acoustic mode softening arises from electrostrictive coupling between polar nanoregions and acoustic modes. X-ray diffraction indicates that the pressure-volume compression curve changes near 2 GPa. © 2010 American Institute of Physics. [doi:10.1063/1.3369278]

I. INTRODUCTION

Lead-based relaxor ferroelectrics with complex perovskite structures exhibit a strong frequency-dispersive dielectric permittivity with broad and smooth temperature dependence.¹ Their high permittivity and high piezoelectric constants make them suitable for applications in devices for sonar or medical imaging.² While extensive theoretical and experimental studies have advanced our understanding of relaxors, their properties are still poorly understood. These difficulties stem from the complexity of these materials, which have a high degree of compositional, structural, and polar disorder.

One of the important recent developments in this field has been the observation that some relaxors transform spontaneously into a ferroelectric phase, as reported for $\text{Pb}(\text{Sc}_{0.5}\text{Ta}_{0.5})\text{O}_3$ and $\text{Pb}(\text{Sc}_{0.5}\text{Nb}_{0.5})\text{O}_3$ (PSN).^{3,4} Dielectric and structural studies have been reported for PSN samples with the degree of disorder controlled by proper high temperature annealing/quenching in different atmospheres.^{5,6} For example, highly ordered PSN samples (with 90% ordering of the Sc and Nb cations on different B sublattices) exhibit a normal paraelectric to ferroelectric transition on cooling.⁵ On the other hand, highly disordered samples first enter a relaxor state on cooling, followed by a cubic relaxor to rhombohedral ferroelectric transition.⁶ These materials are of interest for the study of relaxor properties due to ordering (or disordering) of B-site cations, with corresponding drastic changes in dielectric properties. Several theoretical calculations have been performed on PSN because the ferroelectric ground state is well characterized; these calculations allow for a reliable comparison between theory and experiment. First-

principles based simulations show that chemically ordered regions (COR) are equivalent to or form the nuclei of polar nanoregions (PNRs),⁷ which are central to many of the important properties of relaxors. The current models of relaxor materials, which agree with existing experimental data, invoke the existence of a disordered matrix with COR. In disordered PSN, a first-order phase transition between the relaxor phase and the ferroelectric phase with temperature ($T_c=110\text{ °C}$) has been reported.^{5,6} In its ferroelectric state, disordered PSN has a rhombohedral structure ($R3m$) with displacements of the Pb cation along the threefold axis that have been found to be larger than those for Sc/Nb.^{5,6}

Application of pressure can tune the physical properties of relaxors and introduce new phenomena.⁸⁻¹³ Samara *et al.*⁸⁻¹⁰ pointed out that pressure is an important parameter in the investigations of relaxor-to-ferroelectric crossover phenomena in disordered perovskite systems. The study of pressure and temperature dependencies of the dielectric properties^{14,15} of disordered PSN established its pressure-temperature (P - T) phase diagram. These results and similar studies suggest that PSN represents a typical example of pressure-induced ferroelectric-to-relaxor crossover in lead-based perovskite materials.^{14,15} Motivated by the strong interest in developing a better understanding of the relaxation properties of highly disordered ferroelectrics, we employed high pressure Brillouin and Raman scattering and single crystal x-ray diffraction methods to investigate the high pressure behavior of a single crystal of disordered PSN (D-PSN) from ambient to 12 GPa.

II. EXPERIMENTS

A. High-pressure Raman scattering

Single crystals of D-PSN were grown from a high-temperature solution using a mixture of PbO and B_2O_3 as the

^{a)}Electronic mail: maihaiti@ciw.edu.

^{b)}Deceased.

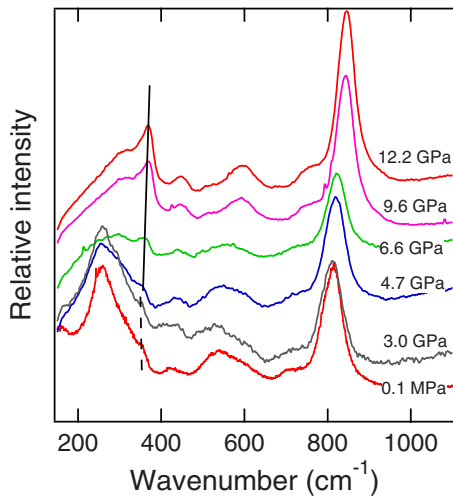


FIG. 1. (Color online) Representative Raman spectra of PSN at selected pressures. Solid and dashed lines indicate where the change has taken place.

solvent.¹⁶ Crystals with dimension of approximately $70 \times 70 \times 20 \mu\text{m}^3$ and orientated along cubic (001) were loaded into a diamond anvil cell (DAC) with neon as the pressure medium. A chip of ruby was included for pressure determination. We employed a Jobin Yvon HR-460 single grating spectrometer with double notch filters with higher throughput but a higher low-frequency cutoff of 80 cm^{-1} as our Raman spectroscopy system. An Ar-ion laser was used as the light source, operating at 514.5 nm with an average incident power of 0.1 W . The scattering geometry was 180° . All spectra were measured at $300 (\pm 1) \text{ K}$ and the average acquisition time was between 10 and 30 s. Figure 1 shows the Raman spectra of a single-crystal of D-PSN at selected pressures. The bands are broad in comparison to the first-order scattering of conventional ferroelectrics, such as PbTiO_3 , which show sharp peaks in their polar phases. We did not measure the low frequency bands (e.g., at 50 cm^{-1}) due to the limitations of the single-grating system used. The sharp peak near the 370 cm^{-1} increases its intensity with pressure above 3 GPa. The linewidth of the band at 550 cm^{-1} also increases with pressure and two of the Raman peaks merge above 4 GPa. We normalized the measured spectra with the Bose–Einstein factor $n(\nu)+1$, where $n(\nu)=1/\exp[h\nu/k_B T - 1]$, where ν is the frequency, h is Planck’s constant, k_B is the Boltzmann constant, and T is the temperature. We then decomposed the measured profiles using a multipeak fitting procedure [Fig. 2(a)]. A reasonable determination of the pressure dependence of each Raman mode could be achieved with the assumption that the peaks are described by spectral functions of damped harmonic oscillators [Fig. 2(b)].

Analyses of the Raman spectra of disordered systems are complicated by the lifting of selection rule due to the disorder. Nevertheless, the main features of the Raman spectrum of D-PSN reflect the Fm-3m symmetry, which is also used as the model for other relaxors such as $\text{Pb}(\text{Zn}_{1/3}\text{Nb}_{2/3})\text{O}_3\text{-PbTiO}_3$ (PZN-PT).¹⁷ The Raman bands can be assigned as follows about 800 cm^{-1} is the A_{1g} band, a fully symmetrical breathing vibration in oxygen octahedra, which is insensitive to pressure. The 550 cm^{-1} band is assigned to the E_g vibration corresponding antiphase breathing

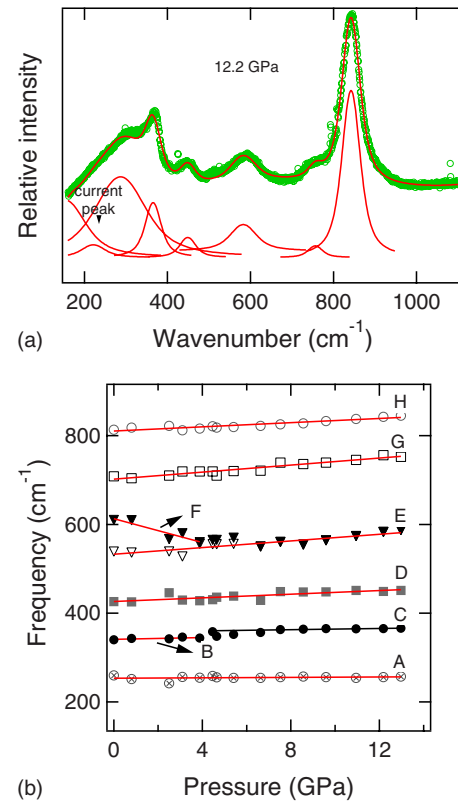


FIG. 2. (Color online) (a) A fit of a Raman spectrum using the sum of the damped harmonic oscillators. (b) Pressure dependencies of Raman bands, marks are data and the capital letters A to H represent the lines of linear fits. The fitting parameters are given as, A: $253.3+0.3P$, B: $340.9+0.9P$, C: $359.6+0.5P$, D: $426.2+2.1P$, E: $532.5+3.7P$, F: $612.9-13.5P$, G: $701.8+4.0P$, H: $810.0+2.4P$, and P is pressure.

of oxygen octahedra. This band splits under tetragonal distortion and is related to the polar distortion. However, pressure suppresses the local polar distortions. We see this in the E_g band with two peaks merging together with pressure. A new peak splits from the 272 cm^{-1} broad band (assigned to F_{2g}), which can be explained by the pressure-induced tilting of octahedra or a lowering of the barriers between the potential wells. Overall, the pressure dependence of the Raman spectrum indicates that a structural phase transition takes place at about 3 GPa.

B. High-pressure Brillouin scattering

A 3+3 pass tandem Fabry–Perot interferometer was employed to investigate the pressure dependence of Brillouin shifts for the D-PSN single crystal in a backscattering geometry. A single frequency Ar^+ ion laser was operated at 514.5 nm and a power of 50 mW . A conventional photon-counting system and a multichannel analyzer were used to detect the signal. A $[001]$ pseudocubic orientated D-PSN single crystal with dimensions of $30 \times 40 \times 30 \mu\text{m}^3$ was loaded into a DAC with Ne as the pressure transmitting medium. A ruby chip was also loaded for pressure determinations

The Brillouin spectra show a pair of peaks corresponding to the quasilongitudinal acoustic mode (L-mode) and a Rayleigh peak at zero frequency (elastic scattering; Fig. 3). The acoustic modes were analyzed with a sum of damped harmonic oscillations. The pressure dependencies of the line-

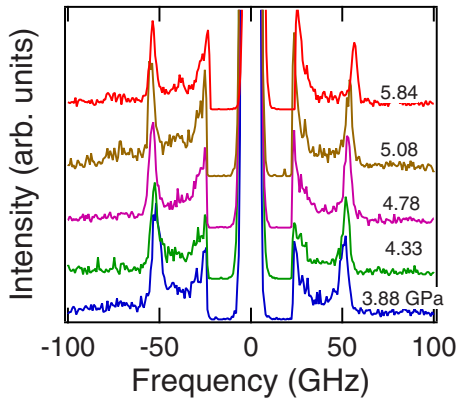


FIG. 3. (Color online) The typical Brillouin spectra at selected pressures. There is one pair of peaks in each spectrum and an additional Rayleigh peak at zero frequency (elastic scattering). The pair of peaks corresponds to the quasilongitudinal acoustic mode (L-mode).

width and frequency of the L-mode are shown in Fig. 4. An elastic anomaly is observed near the transition pressure of 2 GPa. A similar softening of the L-mode upon cooling has also been observed in the PMN-PT, PSN and PZN-PT systems, and can be attributed to the coupling between acoustic mode and PNRs below the so-called Burns temperature.¹⁸ The relaxation process related to the L-mode shows a remarkable slowing down at the transition from the ferroelectric side.

There have been several studies of the coupling between acoustic and relaxation modes in relaxor ferroelectrics such as D-PSN, PMN, and PMN-PT,^{19–21} but previous work has

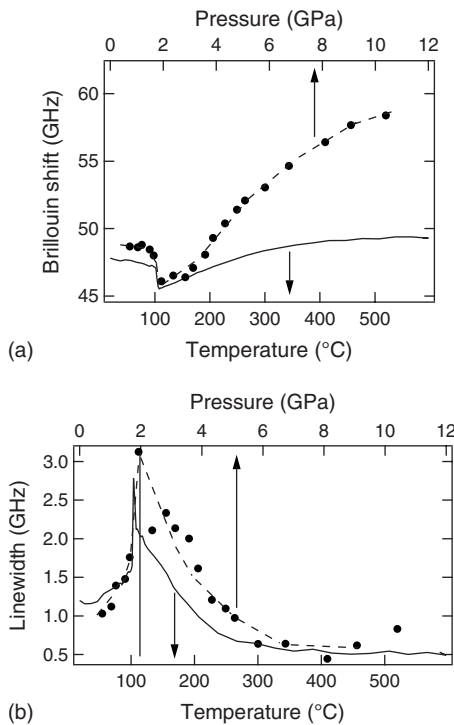


FIG. 4. (a) Pressure dependence of the Brillouin shift of the L-mode (circles). The symbols are data and the dashed curve is a guide to the eyes. For comparison, the temperature dependence of the L-mode (Ref. 21) is also plotted (solid curve). (b) Pressure dependence of the linewidth of the L-mode (solid circle). For comparison, the temperature dependence of the linewidth of the L-mode is also plotted (solid curve).

focused on the temperature effects only. We demonstrate here that pressure has more profound effects. By analogy to the analysis of temperature effects, we find a pressure point where PNRs appear upon decompression, which we call the Burns pressure, P_B . The diffuse scattering and dielectric measurements indicate that relaxor behavior only exists between 1 and 4 GPa in PSN samples at room temperature, thus, $P_B=4$ GPa. We also observed a significant softening of acoustic mode upon decompression similar to that documented for temperature effects in relaxors such as D-PSN or PMN-PT.^{20,21}

It has been suggested that local polarizations fluctuations couple to the acoustic modes via electrorestrictive forces.²⁰ This coupling therefore induces not only a softening in acoustic modes but also increases the linewidth of their excitations (Fig. 4). One can calculate the relaxation time related to this coupling using a Debye-type model:

$$\tau = \frac{\Gamma(P) - \Gamma_\infty}{2\pi(\nu_\infty^2 - \nu^2)}, \quad (1)$$

where ν_∞ is the high-frequency values of the Brillouin shift (Ref. 22), $\Gamma(P)$ is the pressure dependent linewidth, and Γ_∞ is the linewidth at the high-pressure limit about 0.5 GHz. A detailed derivation of the above equation can be found in Ref. 20. It is difficult to obtain ν_∞ independently, because the sound velocity increases rapidly with pressure due to the increased bulk modulus of the D-PSN crystal above 4 GPa. To compare these results with the effects of temperature, we plotted the temperature dependent Brillouin shifts for the L-mode and their linewidths (the experiments were carried out at ambient pressure) in Fig. 4. Pressure and temperature induce very similar relaxation processes.

C. High pressure x-ray diffraction

A (001) orientated D-PSN single crystal with dimensions of $70 \times 70 \times 20 \mu\text{m}^3$, was loaded into the DAC with Ne as the pressure medium and ruby and Au as the pressure gauges. High-energy x-ray diffraction experiments were carried out at beam line BESSRC 11-ID-C of the Advanced Photon Source (Argonne National Laboratory). A premonochromator combined with a Si(311) crystal was employed to provide the monochromatic (115 keV) incident beam with a wavelength close to 0.1077 \AA . An image plate was used as the detector, and gave an instrumental resolution of about 0.005° on the 2θ scale. Typical expose times were between 30 and 60 s. Additional experimental details about the beam-line set up can be found in Ref. 23.

A diffraction pattern was taken at 0.5 GPa at 25°C , and then the temperature was slowly reduced down to 0°C . During this process, several diffraction patterns were taken at different temperatures. Afterwards, the temperature was increased back to 25°C , and the pressure was subsequently increased to the desired values. In this way, we measured the x-ray diffraction patterns up to 14 GPa at room temperature, and up to 10 GPa at 0°C . Because the sample was a (001) oriented single crystal, only the (hk0) indexed Bragg peaks

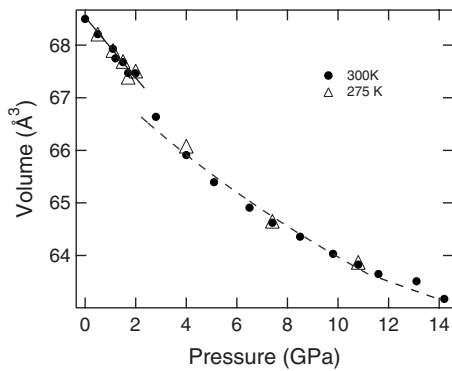


FIG. 5. Pressure volume relations. Solid circles represent the data obtained at 300 K and the open triangles represent the data obtained at 275 K. The Vinet EOS (solid curve) was used to fit the data and yielded a bulk modulus of 119 ± 10 GPa, its pressure derivative of 3.1 ± 0.4 , and initial volume of 68.5 ± 0.2 Å³ below 2 GPa. The fit gives an initial volume of 67.7 ± 0.2 Å³, a bulk modulus of 134 ± 9 GPa and its pressure derivative of 11 above 2 GPa.

were observed. No superlattice peaks were observed in the image, confirming that the sample was mostly disordered in nature.

Together with the crystal structure, the equation of state (EOS) is a fundamental quantity to be measured under pressure. As the EOS of a system describes the relations among the thermodynamics variables of volume, pressure, and temperature; it reflects the underlying structure and bonding of the components involved. Figure 5 shows the pressure dependence of volume for D-PSN samples. A discontinuity is observed in the P - V data around 2 GPa. The Vinet EOS function²⁴ was used to fit the data,

$$P = \frac{3K_0(1-X)}{X^2} \exp\left[\frac{3}{2}(K'_0 - 1)(1-X)\right], \quad (2)$$

where $X=(V/V_0)^{1/3}$, K_0 is the bulk modulus, and K'_0 is its pressure derivative. We fitted the data with two sets of bulk moduli and their pressure derivatives below and above 2 GPa. Below 2 GPa, $V_0=68.5(\pm 0.2)$ Å³, $K_0=119(\pm 10)$ GPa, and $K'_0=3.1(\pm 1.0)$. Above 2 GPa, $V_0=67.4(\pm 0.3)$ Å³, $K_0=196(\pm 12)$ GPa, and $K'_0=11(\pm 2)$. These results indicate that the pressure-volume compression curve changes near the transition point. Considering the bulk moduli of several relaxor ferroelectric materials (e.g., Ref. 25) including 103 GPa for PMN, 105 GPa for PZN-4.5%PT, 69 GPa for PbTiO₃, and 135 GPa for PMN-32%PT, the value of 119 GPa obtained here for D-PSN is typical for relaxor ferroelectrics.

III. DISCUSSION

The ferroelectric transition in D-PSN is not an idealized displacive-type transition due to the coupling of the soft ferroelectric mode with a relaxation mode or PNRs. This coupling between PNRs and the soft ferroelectric mode has been considered as a general feature of lead-perovskite relaxor ferroelectrics. The theoretical description of ferroelectrics of the order-disorder type²⁶ well explained that the coupling between relaxation mode and soft mode would overdamp the soft-mode.

Previously, the highly damped soft mode was observed in PMN system by using neutron scattering,²⁷ and this behavior was attributed to the strong coupling between PNRs and the soft mode (the waterfall effect). Soon after, Stock *et al.*²⁷ observed similar behavior in PMN-60%PT, though the latter material is considered a normal ferroelectrics and not a relaxor. Thus, it is still debatable whether the previously observed “waterfall effect” is associated with the presence of PNRs^{27–30}. However, that a highly damped soft mode (waterfall effect) was observed in PMN-60%PT does not imply that there are no PNRs present. In fact, in PMN- x PT ($x > 50\%$), even though the material exhibits “normal” ferroelectric behavior (sharp ferroelectric phase transition, macroscopic domains, etc.), the (universal) dielectric dispersion²⁸ and central peak (Brillouin scattering),²⁹ characteristic of relaxor polarization have proved to still exist, which implies a contribution from dynamic PNRs (Ref. 29) in these crystals.

In the case of relaxor ferroelectrics, the acoustic mode can couples with PNRs via electrostrictive forces, and such a mechanism is also suggested by several authors (Refs. 29). This coupling will control the pressure or temperature dependence of acoustic modes as observed in our results (Fig. 4). It is interesting to note that in a typical ferroelectric material such as trisarcosine calcium chloride, the temperature dependence of the linewidth shows a sharp peak and Brillouin shifts display a steplike change near the phase transition point.³¹ On the other hand, the Brillouin shifts of relaxor materials show a gradual dependence on temperature or pressure and displays a rather broad peak near the transition point, specially in the relaxor side (for example, D-PSN or Ref. 20).

Recent theoretical studies^{7,32} of the pressure-induced ferroelectric-to-relaxor crossover in chemically disordered PSN suggest that: (1) increasing pressure has a negligible effect on the contribution of chemical disorder or vacancies in a random field; (2) pressure smoothly and monotonically reduces the depths of ferroelectric potential wells, and thus, destabilizes the ferroelectric phase in favor of the relaxor ferroelectric state and the paraelectric phase; (3) reducing the competition from normal ferroelectric ordering corresponds to a relative increase in the random field; and (4) increasing pressure will induce a ferroelectric-to-relaxor phase transition. The P - T phase diagram calculated for PSN qualitatively agrees with that obtained experimentally.

The above hypotheses well explain the pressure-induced ferroelectric to relaxor crossover in complex ABO₃ perovskites, as evidenced by the studies of dielectric spectroscopy, Brillouin scattering, Raman spectroscopy, and x-ray diffraction.^{9,14,15} In general, the measurements can also be interpreted as follows. In mixed perovskites, the chemical disorder from substitution and lattice defects introduce dipoles into the lattice. At very high temperature thermal fluctuations are so large that the dipoles are ill-defined. On cooling, however, the presence of these dipolar entities becomes evident at the Burns temperature T_B . Such dipolar entities are embedded into COR to form PNRs below T_B , enhance the correlations and interactions among them with decreasing T at low pressure and couple them into rapidly growing polar clusters, thereby increasing their coulombic interactions.

Because pressure suppresses the magnitude of the dipoles and the correlations of PNRs, at sufficiently high pressure the correlation of PNRs do not become large enough to permeate the whole sample and to precipitate a ferroelectric transition. Instead, the PNRs exhibit a dynamic “slowing down” of their fluctuations leading to the observed relaxor behavior. It is thus seen that the ferroelectric to relaxor cross-over in complex ABO₃ systems is a unique property of soft ferroelectric mode materials. A comparison of our results with the above model points to some interesting observations. Relaxor materials have a macroaveraged structure (host matrix) and a local structure represented by the PNRs, which tend to couple with acoustic modes via electrostrictive forces and cause the softening of acoustic mode as seen in our measurements. While the Raman bands of relaxor ferroelectrics reflect the local structure related to the PNRs, at the same time they show complex features due to disorder. Pressure suppresses the ferroelectricity and enhances the relaxor behavior at modest pressure as observed here and in other studies.^{7,10,12}

IV. CONCLUSIONS

We report systematic room temperature, high-pressure Brillouin scattering, Raman scattering and x-ray diffraction measurements of D-PSN, a typical relaxor ferroelectric and a model system for understanding the phase transitions in relaxor ferroelectrics and related materials. The pressure-dependent Raman bands are broad, which is a relaxor-specific spectral signature. The Raman spectra indicate a structural phase transition, consistent with the earlier dielectric measurements. We also observed a significant softening in the longitudinal acoustic mode. The similarity of relaxation times found in the temperature and pressure dependencies shows that the softening of longitudinal acoustic mode is attributed to electrostrictive coupling between PNRs and acoustic modes. X-ray diffraction reveals that D-PSN is characterized by two distinct pressure-volume compression curves below and above the phase transition pressure.

ACKNOWLEDGMENTS

We thank S. Gramsch and E. L. Venturini for useful discussions, and R. Yang for help with x-ray diffraction experiments. This work was sponsored by the Office of Naval Research under Grants N00014-02-1-0506, N00014-06-1-0166, and N00014-07-1-0451 and the Carnegie/DOE Alliance Center (CDAC) under Grant DE-FC03-03NA00144. The work at Sandia National Laboratory was supported U.S. Department of Energy under Contract No. DE-AC04-94AL85000. This research also was supported in part by the

Grant-in-Aid for Scientific Research (A), 2005, Grant No. 16204032, and by the 21st Century COE program under MEXT, Japan.

- ¹Z.-G. Ye, *Key Eng. Mater.* **155–156**, 81 (1998); A. Bokov and Z.-G. Ye, *J. Mater. Sci.* **41**, 31 (2006).
- ²S.-E. Park and T. R. Shrout, *J. Appl. Phys.* **82**, 1804 (1997).
- ³F. Chu, N. Setter, and J. Tagantsev, *J. Appl. Phys.* **74**, 5129 (1993).
- ⁴F. Chu, I. M. Reaney, and N. Setter, *J. Appl. Phys.* **77**, 1671 (1995).
- ⁵C. Malibert, B. Dkhil, J. M. Kiat, D. Durand, J. F. Berar, and A. S. Bire, *J. Phys.: Condens. Matter* **9**, 7485 (1997).
- ⁶C. Perrin, N. Menguy, E. Suard, Ch. Muller, C. Caranoni, and A. Stepanov, *J. Phys.: Condens. Matter* **12**, 7523 (2000).
- ⁷B. P. Burton, E. Cockayne, and U. V. Waghmare, *Phys. Rev. B* **72**, 064113 (2005).
- ⁸G. A. Samara, *Phys. Rev. Lett.* **77**, 314 (1996).
- ⁹G. A. Samara, *Phys. Rev. B* **71**, 224108 (2005).
- ¹⁰G. A. Samara, E. L. Venturini, and V. H. Schmidt, *Phys. Rev. B* **63**, 184104 (2001).
- ¹¹J. Kreisel, P. Bouvier, B. Dkhil, P. A. Thomas, A. M. Glazer, T. R. Welberry, B. Chaabane, and M. Mezouar, *Phys. Rev. B* **68**, 014113 (2003).
- ¹²M. Ahart, R. E. Cohen, V. Struzhkin, E. Gregoryanz, D. Rytz, S. A. Prosdandeev, H. K. Mao, and R. J. Hemley, *Phys. Rev. B* **71**, 144102 (2005).
- ¹³P. E. Janolin, B. Dkhil, P. Bouvier, J. Kreisel, and P. A. Thomas, *Phys. Rev. B* **73**, 094128 (2006).
- ¹⁴G. A. Samara and E. L. Venturini, *Phase Transitions* **79**, 21 (2006).
- ¹⁵E. L. Venturini, R. K. Grubbs, G. A. Samara, Y. Bing, and Z.-G. Ye, *Phys. Rev. B* **74**, 064108 (2006).
- ¹⁶Y. Bing and Z.-G. Ye, *J. Cryst. Growth* **250**, 118 (2003).
- ¹⁷F. Jiang and S. Kojima, *Jpn. J. Appl. Phys., Part 1* **38**, 5128 (1999).
- ¹⁸G. Burns and F. H. Dacol, *Solid State Commun.* **48**, 853 (1983).
- ¹⁹F. M. Jiang and S. Kojima, *Phys. Rev. B* **62**, 8572 (2000).
- ²⁰S. Tsukada and S. Kojima, *Phys. Rev. B* **78**, 144106 (2008).
- ²¹M. Ahart, A. Husher, Y. Bing, Z.-G. Ye, R. J. Hemley, and S. Kojima, *Appl. Phys. Lett.* **94**, 142906 (2009).
- ²²S. V. Lishchuk and N. P. Malomuzh, *J. Chem. Phys.* **106**, 6160 (1997).
- ²³U. Rutt, M. A. Beno, J. Stremper, G. Jennings, C. Kurtz, and P. A. Montano, *Nucl. Instrum. Methods Phys. Res. A* **467–468**, 1026 (2001).
- ²⁴P. Vinet, J. Ferrante, J. R. Smith, and J. H. Rose, *J. Phys. C* **19**, L467 (1986).
- ²⁵M. Ahart, A. Asthagiri, Z.-G. Ye, P. Dera, H.-k. Mao, R. E. Cohen, and R. J. Hemley, *Phys. Rev. B* **75**, 144410 (2007).
- ²⁶H. Z. Cummins and A. P. Levanyuk, *Light Scattering Near Phase Transitions* (North-Holland, Amsterdam, 1983).
- ²⁷P. M. Gehring, S. Wakimoto, Z.-G. Ye, and G. Shirane, *Phys. Rev. Lett.* **87**, 277601 (2001); C. Stock, D. Ellis, I. P. Swainson, G. Xu, H. Hiraka, Z. Zhong, H. Luo, X. Zhao, D. Viehland, R. J. Birgeneau, and G. Shirane, *Phys. Rev. B* **73**, 064107 (2006).
- ²⁸A. A. Bokov and Z.-G. Ye, *Mater. Sci. Eng., B* **120**, 206 (2005).
- ²⁹J. H. Ko, S. Kojima, A. A. Bokov, and Z.-G. Ye, *Appl. Phys. Lett.* **91**, 252909 (2007).
- ³⁰A. Naberezhnov, S. Vakhruhev, B. Dorner, D. Strauch, and H. Moudden, *Eur. Phys. J. B* **11**, 13 (1999); C. Stock, H. Luo, D. Viehland, J. F. Li, I. P. Swainson, R. J. Birgeneau, and G. Shirane, *J. Phys. Soc. Jpn.* **74**, 3002 (2005); G. Xu, J. Wen, C. Stock, and P. M. Gehring, *Nature Mater.* **7**, 562 (2008).
- ³¹T. Hikita, P. Schnackenberg, and V. H. Schmidt, *Phys. Rev. B* **31**, 299 (1985).
- ³²S. Tinte, B. P. Burton, E. Cockayne, and U. V. Waghmare, *Phys. Rev. Lett.* **97**, 137601 (2006).